ETH *zürich*

Trion Emission Dominates the Low-Temperature Photoluminescence of CdSe Nanoplatelets

Journal Article

Author(s):
Antolinez, Felipe (ID); Rabouw, Freddy T.; Rossinelli, Aurelio (ID); Keitel, Robert (ID); Cocina, Ario; Becker, Michael A.; Norris, David J. (ID)

Trion Emission Dominates the Low-Temperature Photoluminescence of CdSe Nanoplatelets

Felipe V. Antolinez,[†] Freddy T. Rabouw, [†,§] Aurelio A. Rossinelli,[†] Robert C. Keitel,[†] Ario Cocina,[†] Michael A. Becker,[†,‡] and David J. Norris[,†]*

[†]Optical Materials Engineering Laboratory, Department of Mechanical and Process Engineering, ETH Zurich, 8092 Zurich, Switzerland

[‡]IBM Research Europe – Zurich, Säumerstrasse 4, 8803 Rüschlikon, Switzerland

ABSTRACT. Colloidal nanoplatelets (NPLs) are atomically flat, quasi-two-dimensional particles of a semiconductor. Despite intense interest in their optical properties, several observations concerning the emission of CdSe NPLs remain puzzling. While their ensemble photoluminescence spectrum consists of a single narrow peak at room temperature, two distinct emission features appear at temperatures below ~160 K. Several competing explanations for the origin of this two-color emission have been proposed. Here, we present temperature- and time-dependent experiments demonstrating that the two emission colors are due to two subpopulations of uncharged and charged NPLs. We study dilute films of isolated NPLs, thus excluding any explanation relying on collective effects due to NPL stacking. Temperature-dependent measurements explain that trion emission from charged NPLs is bright at cryogenic temperatures, while temperature activation of nonradiative Auger recombination quenches the trion emission above 160 K. Our findings clarify many of the questions surrounding the photoluminescence of CdSe NPLs.

Colloidal semiconductor nanoplatelets (NPLs) are quasi-two-dimensional particles of semiconductor with an atomically precise thickness.[1] Because of work over the past decade, wet-chemical syntheses can now produce batches of high-quality CdSe NPLs in which all particles have the same thickness,[2] tunable from 2 to 8 monolayers (MLs).[3,4] This well-controlled size in one dimension can then lead to narrower absorption and emission line widths than those observed for spherical CdSe quantum dots (QDs).[5] For 4-ML CdSe NPLs, which is the most commonly studied thickness, the full-width at half-maximum (fwhm) of the emission spectrum at room temperature is less than 35 meV.[5] Such narrow emission lines are desirable for applications such as lighting,[6] displays,[7] and lasers.[8]

However, despite intense interest in the optical properties of CdSe NPLs, several observations concerning their photoluminescence remain puzzling. For example, studies on individual NPLs at room temperature have revealed narrow and spectrally stable emission spectra, but with surprisingly strong fluctuations in the overall intensity on the time scale of seconds.[9] Moreover, NPLs exhibiting bright emission under ambient atmosphere are quenched under vacuum at room temperature, after which the emission turns brighter again with decreasing temperature.[9] Most striking, however, is the temperature dependence of the emission spectrum. At room temperature, the emission spectrum of an ensemble of CdSe NPLs shows a single narrow peak with negligible Stokes shift with respect to the lowest-energy absorption feature.[2,5] In contrast, two distinct emission peaks[10,11] are observed below 160 K, with an energy separation ranging from 18 meV for 5-ML NPLs to 38 meV for 3-ML NPLs.[12]

Efforts to elucidate the origin of this two-color emission from CdSe NPLs have resulted in four contradictory interpretations: (i) band-edge exciton emission with a red-shifted longitudinal-optical-(LO)-phonon replica;[10] (ii) emission from the lowest-energy exciton plus a blue-shifted excited exciton state;[13,14] (iii) emission from individual NPLs plus a red-shifted "excimer" peak from electronically coupled NPL dimers;[15] or (iv) emission from neutral excitons plus red-shifted charged excitons (i.e., trions).[12,16] These competing models have striking qualitative differences. Phonon coupling or excited-exciton emission [interpretations (i) and (ii), respectively] are aspects of the intrinsic photophysics of NPLs and would then presumably produce two-color emission from every

individual NPL. This has not yet been observed in single-NPL experiments.[9] In contrast, in the excimer model [interpretation (iii)], the two-color emission is a collective effect induced, for example, by the assembly of NPLs into stacks. Indeed, the two-color spectrum is known to depend on sample preparation and vary spatially within a sample. The trion-emission model [interpretation (iv)] assumes that a sample contains two subpopulations of neutral and charged NPLs, which each produce one of the two emission colors. Recently, Shornikova *et al.* provided further evidence for this explanation.[16] However, their experiments were performed on NPL films, so collective effects cannot be excluded. Moreover, the implications of trion emission on the temperature dependence of the NPL emission spectrum remain unclear. In particular, an explanation for why only a single emission feature can be observed at room temperature is still needed.

Here, we elucidate the origin of two-color emission from CdSe NPLs at cryogenic temperatures and explain the implications for the room-temperature fluorescence. The observation of two-color emission from films of isolated NPLs, as confirmed by correlated optical spectroscopy and electron microscopy, allows us to exclude the excimer explanation, which relies on interactions between NPLs. Next, photodarkening[17,18] experiments over a duration of a few minutes reveal a rapid decrease of intensity of the low-energy emission feature, while the intensity of the high-energy emission feature stays nearly constant. This behavior indicates that the two emission features are not a consequence of the intrinsic photophysics of the NPLs. Instead, it points to the presence of two distinct subpopulations in the NPL sample. Hence, we conclude that only the trion-emission model is consistent with our experiments. Indeed, temperature-dependent measurements of the two-color spectra support our interpretation and show an exponential temperature activation of nonradiative Auger recombination that quenches the red-shifted emission at room temperature. Our findings clarify many of the open questions surrounding the PL from CdSe NPLs and have broader implications for the temperature-dependent emission behavior of nanocrystals in the weak-confinement limit.

For our experiments, we synthesized 4-ML CdSe NPLs with ~20 × 20 nm lateral size (see Section S1 in the Supporting Information). The reaction is arrested by the injection of Cd(oleate)$_2$, which improves colloidal stability and prevents NPL stacking.[19] This allows us to prepare homogeneous

films of isolated NPLs where all NPLs lie flat on the substrate (i.e. with their wide facets parallel to the surface plane). Such films were produced by spin-coating a dilute dispersion in hexane onto the SiO_2 support film of a transmission electron microscopy grid (Figure 1a). A reference sample containing a thick NPL film was prepared by drop-casting a more concentrated dispersion onto a Si chip with a 3-µm-thick thermal-oxide layer (Figure 1b). See Section S1 in the Supporting Information for a complete description of the sample preparation. The samples were then mounted in a closed-cycle helium cryostat and measured under vacuum. All samples were excited with a 385-nm light-emitting diode (LED), and the emission was recorded with an electron-multiplying charge-coupled-device (EMCCD) camera behind an imaging spectrometer. See Figure S1 and Section S2 in the Supporting Information for further details.

To test whether collective effects are responsible for the two-color emission of CdSe NPLs, we compared the emission spectra obtained from thick drop-cast films and from films of isolated NPLs. Figure 1c shows two emission spectra recorded at a temperature of 4 K close to the sample position depicted in the electron micrograph of Figure 1a (see Section S2 in the Supporting Information for details on how we correlated the two measurements). Both spectra show two clear emission peaks at 2.53 eV (blue arrow) and 2.50 eV (red arrow) plus a weak shoulder at approximately 2.48 eV (gray arrow). As we discuss below, selective photodarkening of the low-energy emission feature (2.50 eV) upon sample illumination causes different relative amplitudes of the emission features for the two spectra. The observation of two-color emission from isolated NPLs (as confirmed by electron microscopy; cf. Figure 1a) indicates that the second emission feature is not due to NPL stacking, as argued by the excimer model [interpretation (iii) above]. Nevertheless, we do observe pronounced differences between the emission spectra of the films of isolated NPLs and thick drop-cast reference samples. Figure 1d shows two normalized PL spectra, recorded at different positions on the thick NPL film. Both spectra contain the same two emission peaks at 2.53 eV (blue arrow) and 2.50 eV (red arrow) as observed from the isolated NPLs but now the lower-energy peak dominates. In addition, the shoulder at 2.48 eV (gray arrow) is significantly stronger than for the isolated NPLs. While the relative amplitudes of the three features varies across the sample, we observe that regions where the NPL film

is somewhat thicker tend to show stronger emission intensity from the two lower-energy features (red and gray arrows). Clearly, while stacking of NPLs (in the film) is not a requirement for the two-color emission (Figure 1c), it does affect the spectrum (Figure 1d). Such effects due to stacking were observed previously, leading to the excimer model.[15] Our measurement (Figure 1c) now shows that two-color emission can occur from a film of isolated NPLs as well.

Previous reports have also examined the relative amplitude of the emission peaks to determine their origin. However, this can clearly depend on the sample preparation[10,15] (cf. Figures 1c,d) and, as shown in very recent photodarkening experiments, changes over a time scale of seconds to minutes.[16] To investigate the time-dependent emission behavior of isolated NPLs without collective effects due to NPL stacking, we recorded a series of emission spectra over 200 s at a temperature of 4 K from our film of isolated NPLs. We illuminated the NPLs with an excitation-power density of ~0.3 W cm^{-2} at a position on the sample that had previously not been illuminated, and each spectral frame was collected with 100-ms exposure time. Thus, the resulting spectral time series in Figure 2a represents the time-dependent emission spectrum from many (~10^5) isolated NPLs simultaneously. While the peak-energy separation stays constant at ~28 meV, the relative emission intensity of the two features changes dramatically over time. To quantify this change, we evaluated the intensity from both peaks separately after background subtraction. In these data (Figure 2b) the intensity of the high-energy emission remains nearly constant during the time of the experiment, while a strong photodarkening of the low-energy emission is observed. This suggests that an intrinsic NPL effect, such as emission from higher-energy excited states due to a phonon bottleneck for thermalization, cannot easily explain the two emission features because bleaching should then affect both peaks equally.

Rather, the observed changes in the two-color emission spectrum are consistent with two subpopulations of NPLs in the sample: uncharged NPLs that produce the high-energy emission and charged NPLs that produce the low-energy emission (see Figure 2c). With polarization-resolved PL measurements under strong magnetic fields, Shornikova et al.[12] showed that the low-energy PL feature in NPLs is indeed consistent with emission from a bright negative-trion ground state. This finding is initially surprising since trion emission is usually not observed from small CdSe QDs.[20] In QDs, where

the charge carriers are strongly confined in all three dimensions, trion emission is usually quenched by nonradiative Auger recombination pathways.[21] In the Auger process, one electron and one hole recombine nonradiatively by exciting a third charge carrier (e.g., the extra electron in the trion) into a higher-energy state through the Coulomb interaction. While this quenches trion emission in QDs, Auger-recombination rates are negligible at cryogenic temperatures for bulk wide-bandgap semiconductors such as CdSe because the Auger process requires momentum conservation.[22] Similarly, Auger recombination should be suppressed in NPLs at cryogenic temperatures, because the trions are only weakly confined by the lateral boundaries of the NPL.

If the low-energy PL feature is indeed due to trion emission, Figure 2b indicates that its intensity rapidly decreases upon photoexcitation. This is in contrast to Shornikova et al.[16] who report an increase in the trion emission. The discrepancy may be due to a different atmosphere in the cryostat (vacuum vs helium vapor) or differences in sample geometry. In particular, our sample preparation method prevents interactions between NPLs and ensures that our measured spectra represent the intrinsic emission efficiencies of the NPL subpopulations. In the NPL films of Shornikova et al.,[16] rapid energy transfer between NPLs[23] can funnel excitations from uncharged to charged NPLs. Moreover, the different environments of NPLs in a film of isolated NPLs compared to a thick film may affect photocharging and discharging. Our experiments also indicate that the intrinsic photodarkening of charged NPLs is stronger than that of uncharged NPLs (Figure 2b). This observation may be rationalized in two ways. First, charged NPLs may be more prone to photochemistry than uncharged NPLs. The occurrence of (occasional) Auger recombination of trions excites the extra charge carrier to a high-energy state. While this excited carrier would usually thermalize quickly on a picosecond time scale, it can also escape the NPL[24] or induce chemical reactions on the surface, leading to defects in charged NPLs that can quench the luminescence. Second, trion emission may be more vulnerable to (charged) surface defects than neutral-exciton emission. When such photoinduced inhomogeneities arise on the NPL surface, the trion may localize there. This introduces high spatial frequency components in the trion wave function, thus enhancing Auger recombination and quenching the emission.[25] Indeed, we have previously observed that even in

CdSe/CdS NPLs with a protective shell, the fluctuating potential-energy landscape produced by surface charges affects the trion emission spectrum and dynamics.[26] Exciton emission, on the other hand, should be only weakly affected by the electrostatic potential of charged surface defects. These two considerations may both contribute to our observation of rapid photodarkening of the trion emission (Figure 2b).

Therefore, based on our experiments, we conclude that the two-color emission at low temperatures is caused by subpopulations of charged and uncharged NPLs. These lead to a trion and exciton emission feature, respectively. However, this then raises the question of how these subpopulations affect the NPL emission at room temperature. Because the relative amplitude of the two emission features is the same for different positions on a fresh film of isolated NPLs that has not been measured previously, we could examine the intensity of the trion and exciton PL as a function of temperature. Figure 3a shows emission spectra from a film of isolated NPLs at different temperatures ranging from 4 to 160 K. At every temperature, we measured at a fresh location on the sample (see Figure S2 in the Supporting Information). We also used spectra that were recorded for no longer than 1 s to minimize the effect of photodarkening. The resulting emission spectra are qualitatively similar to those reported by Tessier *et al.*[10] Both emission peaks shift to lower energy as the temperature increases, and the low-energy emission feature disappears at temperatures above ~160 K.

To quantify the temperature-dependence of the two peaks, we fit each emission spectrum with two Voigt functions. In Figure 3b, the extracted energies of the two peaks show that both shift by ~45 meV as the temperature increases from 4 to 160 K and that their temperature-dependent positions can be well fit with the Varshni relation,[27]

$$E(T) = E_0 - \alpha \frac{T^2}{T+\beta},$$

where α and β are constants. The resulting values from the fit, summarized in Table 1, are similar but slightly larger than the values reported for CdSe bulk and QDs (0.3 to 0.4 meV/K for α and 180 to 320 K for β),[28,29] which could indicate the presence of strain in NPLs.[30] Together with the temperature-independent peak energy separation of $\Delta E_{XT} \approx 28$ meV (Figure 3c), these measurements further

support our assignment of the high-energy peak to ground-state exciton emission and the low-energy feature to trion emission. The trion should shift together with the neutral exciton emission.[31]

As reported previously,[5,10] NPL emission spectra at room temperature consist of only one emission feature. We propose that the temperature dependence of nonradiative Auger rates is responsible for this observation, in analogy to the temperature dependence of Auger recombination in bulk semiconductors.[22] In bulk semiconductors at low temperature, the Auger recombination rate is negligible because of the momentum mismatch between the initial trion state and the final high-energy single-carrier state.[22] At elevated temperatures, the momentum mismatch can be bridged either by thermal excitation of the trion to higher-momentum states (direct Auger recombination) or by coupling to high-momentum phonons of the lattice (indirect Auger recombination). The rate of both types of Auger recombination (direct and phonon-assisted) become much faster at elevated temperature. Because of the weak in-plane confinement of the charge carriers in NPLs, thermal enhancement of the Auger quenching is thus expected to be visible in temperature-dependent measurements of the NPL emission spectrum.

To extract the separate exciton and trion PL emission intensities as a function of temperature (Figure 4a), we integrated the area under each of the two fitted Voigt line shapes from Figure 3a. The exciton emission intensity, I_{Exciton}, varies only by a factor of approximately two across our temperature range, which we ascribe to fluctuations in the NPL sample coverage as we measure at different positions on our films of isolated NPLs. In contrast, the trion emission intensity, I_{Trion}, decreases by about two orders of magnitude as the temperature increases from 4 to 160 K. Figure 4b shows the ratio of trion-to-exciton PL intensity, $I_{\text{Trion}}/I_{\text{Exciton}}$, as a function of temperature. As the temperature increases, $I_{\text{Trion}}/I_{\text{Exciton}}$ decreases monotonically and approximately exponentially, which is consistent with a strong increase in the nonradiative Auger recombination rate of the trion. The high-energy exciton emission likely originates from a temperature-independent subpopulation of uncharged NPLs where no trions are formed. Moreover, these results provide strong evidence for a temperature activation in the Auger recombination rate of the trion and explains why two-color emission is observed at cryogenic temperatures but not at room temperature.

After assigning the low-energy peak in the spectrum to trion emission, we can now speculate about the origin of the lowest-energy feature, which appears as a distinct peak or shoulder (depending on the film thickness) ~19 meV below the trion peak (gray arrows in Figure 1c,d). This splitting is inconsistent with the LO phonon frequency in CdSe (26 meV), ruling out a phonon replica as the origin. By performing the same experiment as in Figure 2 but on thick NPL films (see Figure S3 in the Supporting Information), we observed a simultaneous photodarkening of this lowest-energy feature with the trion emission peak. This suggests that the lowest-energy peak is connected to the trion. We propose that it may be due to a "shakeup" process. This type of emission is not commonly observed in colloidal nanocrystals but under certain conditions can result in multiple emission lines from charged excitons. The shakeup process is a form of *radiative* Auger coupling between one electron in the conduction band and one hole in the valence band with the additional charge carrier. The electron recombines with the hole radiatively while, simultaneously, the additional charge carrier is excited to a higher energy level. In contrast to *nonradiative* Auger recombination, where the third charge carrier accepts all of the recombination energy, in the shakeup process it accepts only a fraction of the energy. Therefore, the PL resulting from a shakeup process is visible at a lower energy than the trion emission peak. The observation of distinct shakeup satellite peaks requires discrete energy levels for the final state of the resident charge carrier. In NPLs, such states exist due to the weak lateral quantum confinement of the charge carriers by the edges of the NPL or by electrostatic potentials due to surface charges.[26] The enhancement of shakeup emission in thick films of NPLs compared to isolated NPLs may result from the different dielectric environment, which affects the electrostatic potential experienced by trions in the NPLs.[26] Alternatively, different NPL orientations or selective reabsorption of the higher-energy features may distort the spectrum recorded from thick films, as previously proposed to explain the enhancement of phonon-assisted exciton emission in samples with stacked NPLs.[10] Shakeup satellites from negative trions, where the final states are higher Landau levels for the electron, have been observed in two-dimensional quantum wells under the influence of a magnetic field.[32,33] Moreover, shakeup emission has been observed in epitaxial InAs/GaAs quantum

dots.[34] However, further investigation is needed to clarify the possible role of shakeup in the emission spectrum of core-only colloidal NPLs.

In addition to the data presented here, the temperature dependence of nonradiative Auger rates is also consistent with results reported by other researchers. The reduction in PL intensity when NPLs are placed under vacuum at room temperature[9] can be attributed to the desorption of smaller molecules such as H_2O and O_2 that reversibly bind to the nanocrystal surface under ambient conditions.[35] These molecules have been shown to passivate surface states that can trap photoexcited charge carriers.[36,37] Thus, the NPLs are more prone to charging under vacuum, which increases nonradiative Auger recombination and, therefore, decreases PL at room temperature. As the samples are cooled, PL is recovered because nonradiative trion recombination becomes prohibited by momentum mismatch.

Trion emission at low temperature is also consistent with measurements that showed a decreasing ratio of low-energy to high-energy PL peaks for decreasing NPL lateral dimensions.[10] This can be explained by the increasing nonradiative Auger rates in laterally small NPLs as high spatial-frequency components contribute to the trion wave functions. Recently, ligand-exchange protocols have enabled the synthesis of CdSe NPLs with significantly higher room-temperature PL quantum efficiencies.[38] We believe that better surface passivation may prevent photoinduced charging of these NPLs and therefore increase their quantum yield due to the absence of extra charge carriers that lead to nonradiative Auger recombination at room temperature.

In summary, we studied the time- and temperature-dependent two-color emission behavior of electronically isolated CdSe NPLs. We find that radiative trion emission is responsible for the low-energy emission feature at ~28 meV below the exciton state. Because we examine films of isolated NPLs, we can rule out any collective effect due to NPL stacking. The trion emission is bright at cryogenic temperatures because weak lateral confinement of trions suppresses nonradiative Auger recombination due to the in-plane momentum mismatch with the final state. Photoinduced creation of surface defects or trapped charges, however, lead to a prominent increase of the Auger rates at low temperature on the time scale of seconds to minutes. Temperature-dependent PL spectra confirm our interpretation and show an exponential dependence of the trion-to-exciton PL ratio. Identifying

strategies to suppress charging could therefore be an essential step toward increasing the PL QY of colloidal nanocrystals in the weak-confinement regime.

ASSOCIATED CONTENT

Supporting Information

The Supporting Information is available free of charge on the ACS Publications website at DOI: 10.1021/xxxxxxx.

A detailed description of the sample fabrication, the optical setup, and additional optical data.

AUTHOR INFORMATION

Corresponding Author

*Email: dnorris@ethz.ch.

ORCID

Felipe V. Antolinez: 0000-0002-1787-0112

Freddy T. Rabouw: 0000-0002-4775-0859

Aurelio A. Rossinelli: 0000-0001-6930-4190

Robert C. Keitel: 0000-0002-9412-8034

Ario Cocina: 0000-0003-1560-5849

Michael A. Becker: 0000-0003-2042-9384

David J. Norris: 0000-0002-3765-0678

Present Address

§Debye Institute for Nanomaterials Science, Utrecht University, Princetonplein 1, 3584 CC Utrecht, The Netherlands.

Rubicon Grant 680-50-1509) and the SNSF QuantERA project RouTe (grant no. 20QT21_175389), respectively.

REFERENCES

(1)   Ithurria, S.; Dubertret, B. Quasi 2D Colloidal CdSe Platelets with Thicknesses Controlled at the Atomic Level. *J. Am. Chem. Soc.* **2008**, *130*, 16504–16505.

(2)   Riedinger, A.; Ott, F. D.; Mule, A.; Mazzotti, S.; Knüsel, P. N.; Kress, S. J. P.; Prins, F.; Erwin, S. C.; Norris, D. J. An Intrinsic Growth Instability in Isotropic Materials Leads to Quasi-Two-dimensional Nanoplatelets. *Nat. Mater.* **2017**, *16*, 743–749.

(3)   Cho, W.; Kim, S.; Coropceanu, I.; Srivastava, V.; Diroll, B. T.; Hazarika, A.; Fedin, I.; Galli, G.; Schaller, R. D.; Talapin, D. V. Direct Synthesis of Six-Monolayer (1.9 nm) Thick Zinc-Blende CdSe Nanoplatelets Emitting at 585 nm. *Chem. Mater.* **2018**, *30*, 6957–6960.

(4)   Christodoulou, S.; Climente, J. I.; Planelles, J.; Brescia, R.; Prato, M.; Martín-Garciá, B.; Khan, A. H.; Moreels, I. Chloride-Induced Thickness Control in CdSe Nanoplatelets. *Nano Lett.* **2018**, *18*, 6248–6254.

(5)   Ithurria, S.; Tessier, M. D.; Mahler, B.; Lobo, R. P. S. M.; Dubertret, B.; Efros, Al. L. Colloidal Nanoplatelets with Two-Dimensional Electronic Structure. *Nat. Mater.* **2011**, *10*, 936–941.

(6)   Chen, Z.; Nadal, B.; Mahler, B.; Aubin, H.; Dubertret, B. Quasi-2D Colloidal Semiconductor Nanoplatelets for Narrow Electroluminescence. *Adv. Funct. Mater.* **2014**, *24*, 295–302.

(7)   Cunningham, P. D.; Souza, J. B.; Fedin, I.; She, C.; Lee, B.; Talapin, D. V. Assessment of Anisotropic Semiconductor Nanorod and Nanoplatelet Heterostructures with Polarized Emission for Liquid Crystal Display Technology. *ACS Nano* **2016**, *10*, 5769–5781.

(8)   Grim, J. Q.; Christodoulou, S.; Di Stasio, F.; Krahne, R.; Cingolani, R.; Manna, L.; Moreels, I. Continuous-Wave Biexciton Lasing at Room Temperature Using Solution-Processed Quantum Wells. *Nat. Nanotechnol.* **2014**, *9*, 891–895.

(9)   Tessier, M. D.; Javaux, C.; Maksimovic, I.; Loriette, V.; Dubertret, B. Spectroscopy of Single

CdSe Nanoplatelets. *ACS Nano* **2012**, *6*, 6751–6758.

(10)   Tessier, M. D.; Biadala, L.; Bouet, C.; Ithurria, S.; Abecassis, B.; Dubertret, B. Phonon Line Emission Revealed by Self-Assembly of Colloidal Nanoplatelets. *ACS Nano* **2013**, *7*, 3332–3340.

(11)   Biadala, L.; Liu, F.; Tessier, M. D.; Yakovlev, D. R.; Dubertret, B.; Bayer, M. Recombination Dynamics of Band Edge Excitons in Quasi-Two- Dimensional CdSe Nanoplatelets. *Nano Lett.* **2014**, *14*, 1134–1139.

(12)   Shornikova, E. V.; Biadala, L.; Yakovlev, D. R.; Sapega, V. F.; Kusrayev, Y. G.; Mitioglu, A. A.; Ballottin, M. V.; Christianen, P. C. M.; Belykh, V. V.; Kochiev, M. V.; Sibeldin, N. N.; Golovatenko, A. A.; Rodina, A. V.; Gippius, N. A.; Kuntzmann, A.; Jiang, Y.; Nasilowski, M.; Dubertret, B.; Bayer, M. Addressing the Exciton Fine Structure in Colloidal Nanocrystals: The Case of CdSe Nanoplatelets. *Nanoscale* **2018**, *10*, 646–656.

(13)   Achtstein, A. W.; Scott, R.; Kickhöfel, S.; Jagsch, S. T.; Christodoulou, S.; Bertrand, G. H. V.; Prudnikau, A. V.; Antanovich, A.; Artemyev, M.; Moreels, I.; Schliwa, A.; Woggon, U. P-State Luminescence in CdSe Nanoplatelets: Role of Lateral Confinement and a Longitudinal Optical Phonon Bottleneck. *Phys. Rev. Lett.* **2016**, *116*, 116802.

(14)   Specht, J. F.; Scott, R.; Corona Castro, M.; Christodoulou, S.; Bertrand, G. H. V.; Prudnikau, A. V.; Antanovich, A.; Siebbeles, L. D. A.; Owschimikow, N.; Moreels, I.; Artemyev, M.; Woggon, U.; Achtstein, A. W.; Richter, M. Size-Dependent Exciton Substructure in CdSe Nanoplatelets and Its Relation to Photoluminescence Dynamics. *Nanoscale* **2019**, *11*, 12230–12241.

(15)   Diroll, B. T.; Cho, W.; Coropceanu, I.; Harvey, S. M.; Brumberg, A.; Holtgrewe, N.; Crooker, S. A.; Wasielewski, M. R.; Prakapenka, V. B.; Talapin, D. V.; Schaller, R. D. Semiconductor Nanoplatelet Excimers. *Nano Lett.* **2018**, *18*, 6948–6953.

(16)   Shornikova, E. V.; Yakovlev, D. R.; Biadala, L.; Crooker, S. A.; Belykh, V. V.; Kochiev, M. V.; Kuntzmann, A.; Nasilowski, M.; Dubertret, B.; Bayer, M. Negatively Charged Excitons in CdSe Nanoplatelets. *Nano Lett.* **2020**, *20*, 1370–1377.

(17) Brokmann, X.; Hermier, J.-P.; Messin, G.; Desbiolles, P.; Bouchaud, J.-P.; Dahan, M. Statistical Aging and Nonergodicity in the Fluorescence of Single Nanocrystals. *Phys. Rev. Lett.* **2003**, *90*, 120601.

(18) Chung, I.; Bawendi, M. G. Relationship between Single Quantum-Dot Intermittency and Fluorescence Intensity Decays from Collections of Dots. *Phys. Rev. B* **2004**, *70*, 165304.

(19) Singh, S.; Tomar, R.; ten Brinck, S.; De Roo, J.; Geiregat, P.; Martins, J. C.; Infante, I.; Hens, Z. Colloidal CdSe Nanoplatelets, A Model for Surface Chemistry/Optoelectronic Property Relations in Semiconductor Nanocrystals. *J. Am. Chem. Soc.* **2018**, *140*, 13292–13300.

(20) Efros, Al. L.; Rosen, M. Random Telegraph Signal in the Photoluminescence Intensity of a Single Quantum Dot. *Phys. Rev. Lett.* **1997**, *78*, 1110–1113.

(21) Cragg, G. E.; Efros, Al. L. Suppression of Auger Processes in Confined Structures. *Nano Lett.* **2010**, *10*, 313–317.

(22) Abakumov, V. N.; Perel, V. I.; Yassievich, I. N. *Nonradiative Recombination in Semiconductors*; Elsevier: Amsterdam, NL, 1991.

(23) Rowland, C. E.; Fedin, I.; Zhang, H.; Gray, S. K.; Govorov, A. O.; Talapin, D. V; Schaller, R. D. Picosecond Energy Transfer and Multiexciton Transfer Outpaces Auger Recombination in Binary CdSe Nanoplatelet Solids. *Nat. Mater.* **2015**, *14*, 484–489.

(24) Shabaev, A.; Efros, Al. L.; Efros, A. L. Dark and Photo-Conductivity in Ordered Array of Nanocrystals. *Nano Lett.* **2013**, *13*, 5454–5461.

(25) Kharchenko, V. A.; Rosen, M. Auger Relaxation Processes in Semiconductor Nanocrystals and Quantum Wells. *J. Lumin.* **1996**, *70*, 158–169.

(26) Antolinez, F. V; Rabouw, F. T.; Rossinelli, A. A.; Cui, J.; Norris, D. J. Observation of Electron Shakeup in CdSe/CdS Core/Shell Nanoplatelets. *Nano Lett.* **2019**, *19*, 8495–8502.

(27) Varshni, Y. P. Temperature Dependence of the Energy Gap in Semiconductors. *Physica* **1967**, *34*, 149–154.

(28) Valerini, D.; Cretí, A.; Lomascolo, M.; Manna, L.; Cingolani, R.; Anni, M. Temperature Dependence of the Photoluminescence Properties of Colloidal CdSe∕ZnS Core/Shell Quantum

Dots Embedded in a Polystyrene Matrix. *Phys. Rev. B* **2005**, *71*, 1–6.

(29)   Al Salman, A.; Tortschanoff, A.; Mohamed, M. B.; Tonti, D.; van Mourik, F.; Chergui, M. Temperature Effects on the Spectral Properties of Colloidal CdSe Nanodots, Nanorods, and Tetrapods. *Appl. Phys. Lett.* **2007**, *90*, 093104.

(30)   Zhu, Z.; Zhang, A.; Ouyang, G.; Yang, G. Band Gap Tunability in Semiconductor Nanocrystals by Strain: Size and Temperature Effect. *J. Phys. Chem. C* **2011**, *115*, 6462–6466.

(31)   Ross, J. S.; Wu, S.; Yu, H.; Ghimire, N. J.; Jones, A. M.; Aivazian, G.; Yan, J.; Mandrus, D. G.; Xiao, D.; Yao, W.; Xu, X. Electrical Control of Neutral and Charged Excitons in a Monolayer Semiconductor. *Nat. Commun.* **2013**, *4*, 1474.

(32)   Nash, K. J.; Skolnick, M. S.; Saker, M. K.; Bass, S. J. Many Body Shakeup in Quantum Well Luminescence Spectra. *Phys. Rev. Lett.* **1993**, *70*, 3115–3118.

(33)   Finkelstein, G.; Shtrikman, H.; Bar-Joseph, I. Shakeup Processes in the Recombination Spectra of Negatively Charged Excitons. *Phys. Rev. B* **1996**, *53*, 12593–12596.

(34)   Paskov, P. P.; Holtz, P. O.; Wongmanerod, S.; Monemar, B.; Garcia, J. M.; Schoenfeld, W. V; Petroo, P. M. Auger Processes in InAs Self-Assembled Quantum Dots. *Phys. E* **2000**, *6*, 440–443.

(35)   Gómez, D. E.; Van Embden, J.; Mulvaney, P.; Fernée, M. J.; Rubinsztein-Dunlop, H. Exciton-Trion Transitions in Single CdSe-CdS Core-Shell Nanocrystals. *ACS Nano* **2009**, *3*, 2281–2287.

(36)   Cordero, S. R.; Carson, P. J.; Estabrook, R. A.; Strouse, G. F.; Buratto, S. K. Photo-Activated Luminescence of CdSe Quantum Dot Monolayers. *J. Phys. Chem. B* **2000**, *104*, 12137–12142.

(37)   Ladizhansky, V.; Hodes, G.; Vega, S. Solid State NMR Study of Water Binding on the Surface of CdS Nanoparticles. *J. Phys. Chem. B* **2000**, *104*, 1939–1943.

(38)   Dufour, M.; Qu, J.; Greboval, C.; Méthivier, C.; Lhuillier, E.; Ithurria, S. Halide Ligands To Release Strain in Cadmium Chalcogenide Nanoplatelets and Achieve High Brightness. *ACS Nano* **2019**, *13*, 5326–5334.

	E_0	α	β
High-energy feature	2.5030 ± 0.0001 eV	0.65 ± 0.03 meV/K	216 ± 17 K
Low-energy feature	2.5308 ± 0.0002 eV	0.80 ± 0.07 meV/K	283 ± 39 K

Table 1. Values from the fit of the Varshni relation $E(T) = E_0 - \alpha T^2/(\beta + T)$ to the temperature-dependent NPL emission spectra from Figure 3a. The fits are shown as dashed lines in Figure 3b.
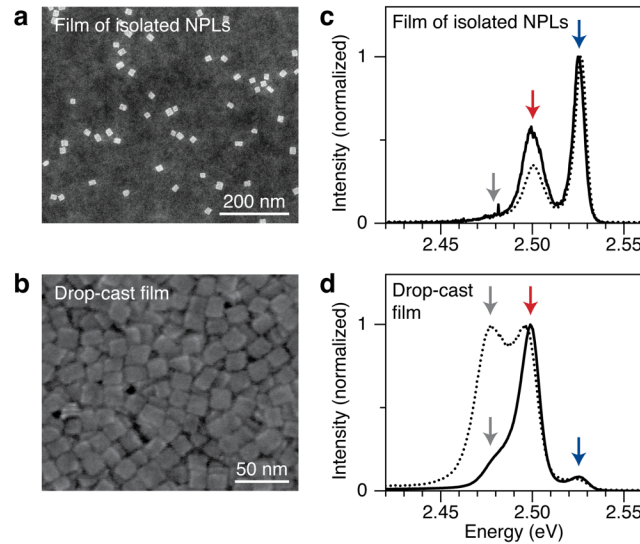
Figure 1. Low-temperature photoluminescence from films of isolated NPLs and drop-cast NPL films. (a) Scanning transmission electron micrograph of a film of isolated NPLs prepared by spin-coating a dilute dispersion of square 4-ML NPLs (~20×20 nm lateral dimensions) onto a TEM grid. The bright spots in the image are individual NPLs. (b) Scanning electron microscopy (SEM) image of a thick film prepared by drop-casting the stock dispersion onto a Si chip. On these samples, NPL stacking is clearly observed across the whole sample. Prior to imaging, the sample was dipped in methyl acetate to remove excess ligands and facilitate SEM imaging. (c) Two photoluminescence spectra from films of isolated NPLs measured close to the sample position shown in panel a at 4 K. The spectra consist of two dominant emission peaks at ~2.53 eV (blue arrow) and ~2.50 eV (red arrow), and a shoulder at ~2.48 eV (gray arrow). (d) Two photoluminescence spectra at 4 K recorded at positions with different film thickness on a drop-cast NPL film. The spectra consist of either two emission peaks and a shoulder (solid line) or three emission peaks (dotted line). The features are at the same position as those in the spectra in panel c.
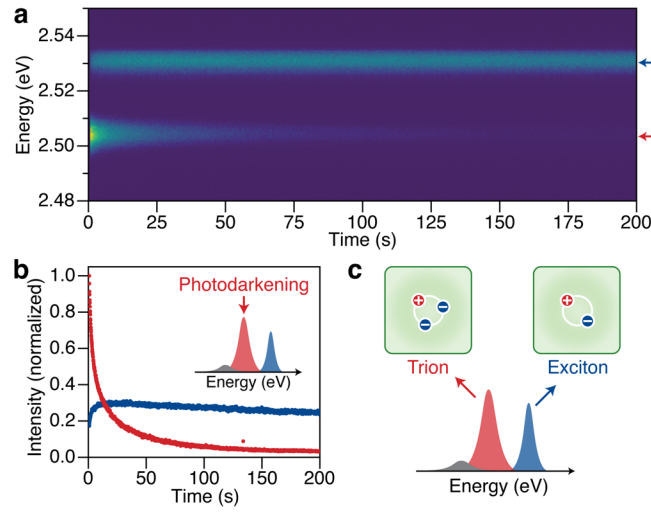
Figure 2. Photodarkening of the trion and exciton emission. (a) Emission time series at 4 K for a film of isolated NPLs, where each vertical spectral frame is accumulated over 100 ms. Intensity is shown as a color scale in arbitrary units. The high- and low-energy emission features are indicated by the blue and red arrows, respectively. (b) Time-dependence of the total photoluminescence intensity from the exciton (blue) and trion (red) from the time series shown in panel a. (c) When a NPL is charged and an additional charge carrier is present in the nanocrystal, the photoexcited electron–hole pair can bind to the delocalized charge to form a trion. At low temperatures, photoluminescence from the trion state can be observed as a distinct emission feature that lies energetically below the exciton emission peak.
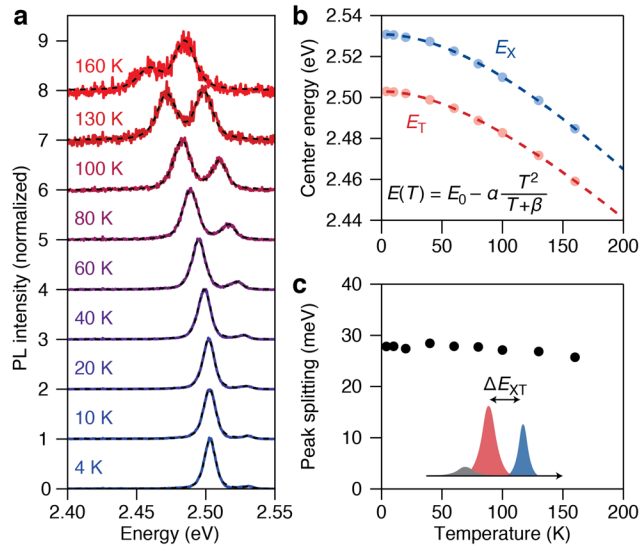
Figure 3. Temperature-dependence of the trion and exciton emission features with energies E_T and E_X, respectively. (a) Normalized photoluminescence spectra recorded from the same sample of isolated NPLs studied in Figure 2. Each spectrum was integrated for no more than 1 s to minimize the effect of photodarkening. The black dashed lines are the result from fitting two Voigt line shapes to the spectra. (b) Resulting peak energies from the Voigt fit to the data in panel a. Both the exciton (blue) and trion (red) emission can be well fit by the Varshni relation as shown by the dashed lines. (c) Energy separation ΔE_{XT} between the exciton and trion emission features as a function of temperature.
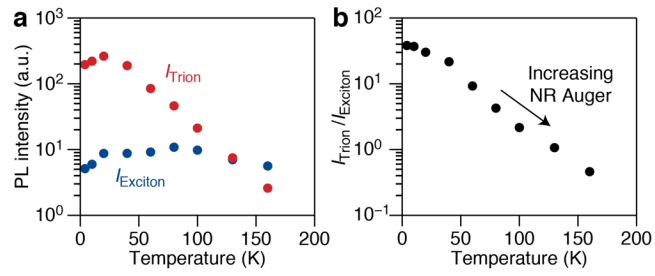
Figure 4. Temperature dependence of the trion and exciton emission intensity. (a) Absolute intensity of the exciton (blue) and trion (red) emission as a function of temperature. (b) Intensity ratio, $I_{\mathrm{Trion}}/I_{\mathrm{Exciton}}$, between the trion and exciton emission peaks from panel a.

TABLE OF CONTENTS GRAPHIC